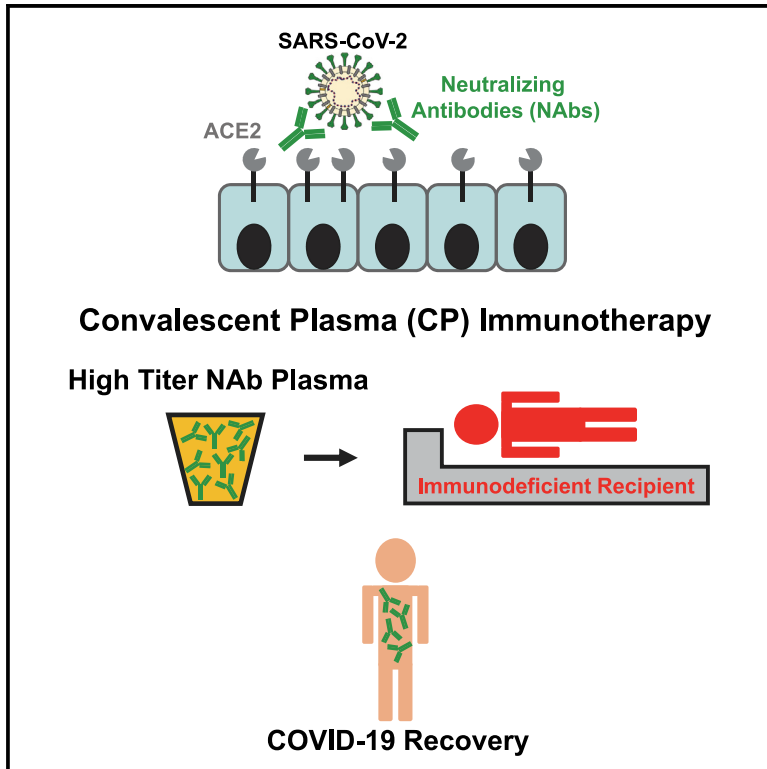


Convalescent plasma-mediated resolution of COVID-19 in a patient with humoral immunodeficiency

Graphical Abstract



Authors

Kazuhito Honjo, Ronnie M. Russell, Ran Li, ..., Sonya L. Heath, Beatrice H. Hahn, Randall S. Davis

Correspondence

bhahn@penmedicine.upenn.edu (B.H.H.),
rsdavis@uab.edu (R.S.D.)

In Brief

An immunodeficient patient with protracted COVID-19 unable to mount a humoral immune response rapidly recovered following transfusion with convalescent plasma. Honjo et al. found that immunotherapy with high-titer neutralizing antibodies was clinically beneficial. However, since neutralizing activity of convalescent plasmas varies widely, units should be tested prior to therapy.

Highlights

- Convalescent plasma clinically benefited a severely ill immunodeficient patient
- The transfer of high-titer neutralizing antibodies led to rapid clinical recovery
- Neutralizing activity was low in most convalescent plasmas but high in recipients
- Neutralizing activity should be tested in both plasma donors and recipients



Report

Convalescent plasma-mediated resolution of COVID-19 in a patient with humoral immunodeficiency

Kazuhiro Honjo,^{1,13} Ronnie M. Russell,^{2,3,13} Ran Li,¹ Weimin Liu,² Regina Stoltz,² Edlue M. Tabengwa,¹ Yutao Hua,¹ Lynn Prichard,¹ Ashton N. Kornbrust,⁴ Sarah Sterrett,¹ Marisa B. Marques,⁴ Jose L. Lima,⁴ Chris M. Lough,⁵ Todd P. McCarty,¹ Thomas J. Ketas,⁶ Theodora Hatzioannou,⁷ Paul D. Bieniasz,^{7,8} David T. Redden,⁹ John P. Moore,⁶ Paul A. Goepfert,^{1,10} Sonya L. Heath,^{1,10} Beatrice H. Hahn,^{2,3,*} and Randall S. Davis^{1,10,11,12,14,*}

¹Department of Medicine, University of Alabama at Birmingham, Birmingham, AL 35294, USA

²Department of Medicine, University of Pennsylvania, Philadelphia, PA 19104, USA

³Department of Microbiology, University of Pennsylvania, Philadelphia, PA 19104, USA

⁴Department of Pathology, University of Alabama at Birmingham, Birmingham, AL 35294, USA

⁵LifeSouth Community Blood Centers, Gainesville, FL 32607, USA

⁶Department of Microbiology and Immunology, Weill Medical College of Cornell University, New York, NY 10065, USA

⁷Laboratory of Retrovirology, The Rockefeller University, New York, NY 10028, USA

⁸Howard Hughes Medical Institute, The Rockefeller University, New York, NY 10028, USA

⁹Department of Biostatistics, University of Alabama at Birmingham, Birmingham, AL 35294, USA

¹⁰Department of Microbiology, University of Alabama at Birmingham, Birmingham, AL 35294, USA

¹¹Department of Biochemistry & Molecular Genetics, University of Alabama at Birmingham, Birmingham, AL 35294, USA

¹²Comprehensive Cancer Center, University of Alabama at Birmingham, Birmingham, AL 35294, USA

¹³These authors contributed equally

¹⁴Lead contact

*Correspondence: bhahn@penntermine.upenn.edu (B.H.H.), rsdavis@uab.edu (R.S.D.)

<https://doi.org/10.1016/j.xcrm.2020.100164>

SUMMARY

Convalescent plasma (CP) is widely used to treat COVID-19, but without formal evidence of efficacy. Here, we report the beneficial effects of CP in a severely ill COVID-19 patient with prolonged pneumonia and advanced chronic lymphocytic leukemia (CLL), who was unable to generate an antiviral antibody response of her own. On day 33 after becoming symptomatic, the patient received CP containing high-titer (ID₅₀ > 5,000) neutralizing antibodies (NAbs), defervesced, and improved clinically within 48 h and was discharged on day 37. Hence, when present in sufficient quantities, NAbs to SARS-CoV-2 have clinical benefit even if administered relatively late in the disease course. However, analysis of additional CP units revealed widely varying NAb titers, with many recipients exhibiting endogenous NAb responses far exceeding those of the administered units. To obtain the full therapeutic benefits of CP immunotherapy, it will thus be important to determine the neutralizing activity in both CP units and transfusion candidates.

INTRODUCTION

One strategy to treat coronavirus disease 2019 (COVID-19) is to use convalescent plasma (CP) from individuals who have successfully cleared severe acute respiratory syndrome coronavirus 2 (SARS-CoV-2) infections and established humoral immunity.¹ Historical evidence indicates that CP mitigates human infectious diseases,² including those caused by the related SARS-CoV-1 (SARS) and Middle East respiratory syndrome (MERS) coronaviruses.^{3,4} CP therapy is widely used and was initiated as an investigational new drug (IND) by the US Food and Drug Administration (FDA) through a nationwide expanded access treatment protocol.⁵ Considered safe,^{6,7} it was approved for emergency use authorization (EUA) on August 23, 2020.⁸ However, as of yet there is no evidence for efficacy,^{9–12} thus rendering this deci-

sion controversial.¹³ This may be because correlates of immune protection are lacking, which render the identification of appropriate convalescing donors and recipients difficult. A key component of CP is neutralizing antibodies (NAbs) that impede SARS-CoV-2 entry into human cells, usually by inhibiting nanomolar affinity interactions between the receptor-binding domain (RBD) of the viral spike (S-protein) and the angiotensin-converting enzyme 2 (ACE2) receptor.^{14,15} Recent reports indicate, but do not prove, that CPs containing high NAb titers can be beneficial when administered within a few days of hospitalization.^{9–11} Given later or in lower amounts, CP NAbs may be unable to meaningfully supplement endogenous NAbs produced during seroconversion.

Here, we report the successful administration of CP to a COVID-19 patient who was unable to generate her own antiviral



A Clinical Course of the Patient

Days after symptom onset (DPO)	-23	-16	-9	0	8	19	20	24	27	28	29	30	31	32	33	34	35	36	37	59	85	119	
Symptoms		Exposure to relative		Cough	Cough; Fever	Cough; Fever 38.8°C; Dyspnea SpO2 86%		Cough	Fever 39°C and Anorexia	Fever, Cough, Headache, and Dyspnea									Defervescence and improved appetite				
Diagnostics					PCR+	CT: Ground glass PNA			CT: Bilateral PNA CXR: Interstitial PNA	PCR+									PCR-			CXR: PNA resolved	
Interventions	Obinutuzumab			IVIg		Hydroxychloroquine		IVIg	Piperacillin-tazobactam and Supplemental O2														
Hospitalization						Admission	Discharge			Admission												Discharge	
Weight (kg)	61.3					61.8			54.6						53.1							62.8	63.3

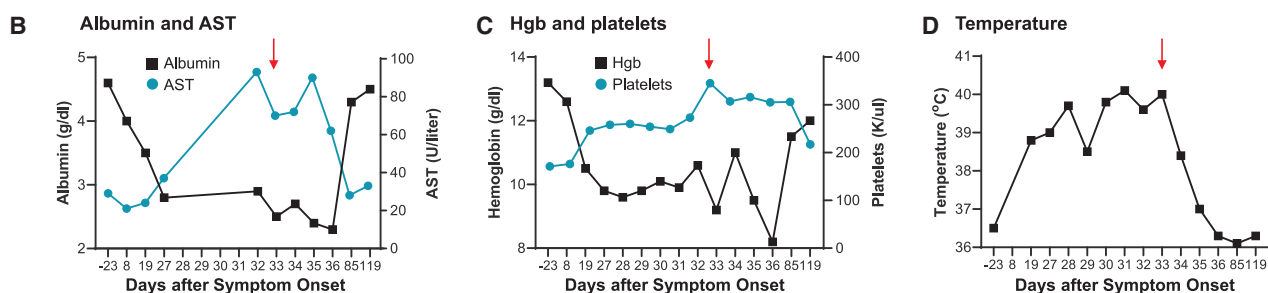


Figure 1. Timeline of exposure and clinical course of the patient

(A) SARS-CoV-2 infection was diagnosed by quantitative real-time polymerase chain reaction (PCR) of respiratory swab samples (A). Notable symptoms at days post onset (DPO), hospitalization course, relevant interventions, and body weight are indicated. IVIg denotes intravenous immunoglobulin; CT, computed tomography; PNA, pneumonia; CXR, chest radiograph; CP, convalescent plasma.

(B–D) Longitudinal analysis of serum albumin and aspartate aminotransferase (AST) (B), hemoglobin and platelet counts (C), and maximum body temperatures (D) are shown after symptom onset. The date of CP infusion (B–D) is indicated by a red arrow.

antibodies (Abs) due to underlying B cell chronic lymphocytic leukemia (CLL). The CP contained high-titer NAb (ID₅₀ >5,000) and was given on day 33 after symptom onset. Her prolonged clinical illness and fever resolved rapidly and she was discharged 4 days later, providing compelling evidence for a curative antiviral effect of the administered NAb, even though they were given late in the disease course. To place this case in context, we quantified NAb titers in additional banked and remnant CP units used to treat COVID-19 patients at the University of Alabama at Birmingham (UAB), as well as in CP recipients before and after transfusion. Many CP units from convalescent donors had only low-titer NAb and thus were unable to usefully supplement endogenously produced Abs post-seroconversion.

RESULTS

Presentation of the case and clinical course

A 72-year-old female with a 20-year history of CLL developed a dry cough following exposure to her daughter (relative 1) who had contracted COVID-19 (Figure 1). The patient had a history of humoral immunodeficiency with chronic sinopulmonary infections requiring monthly intravenous immunoglobulin (IVIg) infusions for over 4 years. Given the progression of her CLL with Rai stage III disease in December 2019, obinutuzumab anti-CD20 B cell depletion immunotherapy was initiated. Her last treatment was 23 days before symptom onset and she had received IVIg 9 days earlier. Relative 1 developed a dry cough 17 days after a holiday in Key West, FL (Figure S1A), presented to a local hospital with headache, ageusia, and diarrhea, tested

positive for SARS-CoV-2 by polymerase chain reaction (PCR) analysis of a respiratory swab 11 days post-symptom onset (DPO), and was admitted with fever, dyspnea, and psychataxia. Her spouse (relative 2), who had also traveled, developed myalgia and headache, and was SARS-CoV-2 virus positive on DPO 8 (Figure S1B). With worsening cough and fever, he was admitted from DPO 10–15. Following exposure to relative 1, the CLL patient tested positive for SARS-CoV-2 virus on DPO 8 (Figure 1). She was admitted on DPO 19 with dyspnea and an oxygen saturation of 86% on ambient air. Computed tomography angiography (CTA) showed ground glass opacities consistent with COVID-19-related pneumonia (Figure 2A). After 24 h, she was discharged on hydroxychloroquine. Despite receiving an IVIg infusion at DPO 24, she developed worsening dyspnea, fever, and loss of appetite with a 7.2-kg (15.8-lb) weight loss and was re-admitted on DPO 27. Laboratory studies showed albumin of 2.8 g per deciliter (reference range, 3.4–4.8), ferritin of 521.8 ng per milliliter (reference range, 4.6–204), high-sensitivity C-reactive protein of 67.2 mg per liter (reference range, ≤0.6), and fibrinogen of 729 mg per deciliter (reference range, 200–400). Repeat chest CTA and radiography (Figures 2B and 2C) revealed worsening bilateral infiltrates concerning for bacterial superinfection and piperacillin-tazobactam was started. A repeat SARS-CoV-2 PCR test was positive, indicating persistent infection. She remained febrile to 40°C, with poor nutrition status, elevated transaminases, and anemia (Figures 1B and 1C). Following their recovery, her relatives visited a blood donation center. Relative 2 had a complementary O Rh positive blood type. CP was designated for the patient, who

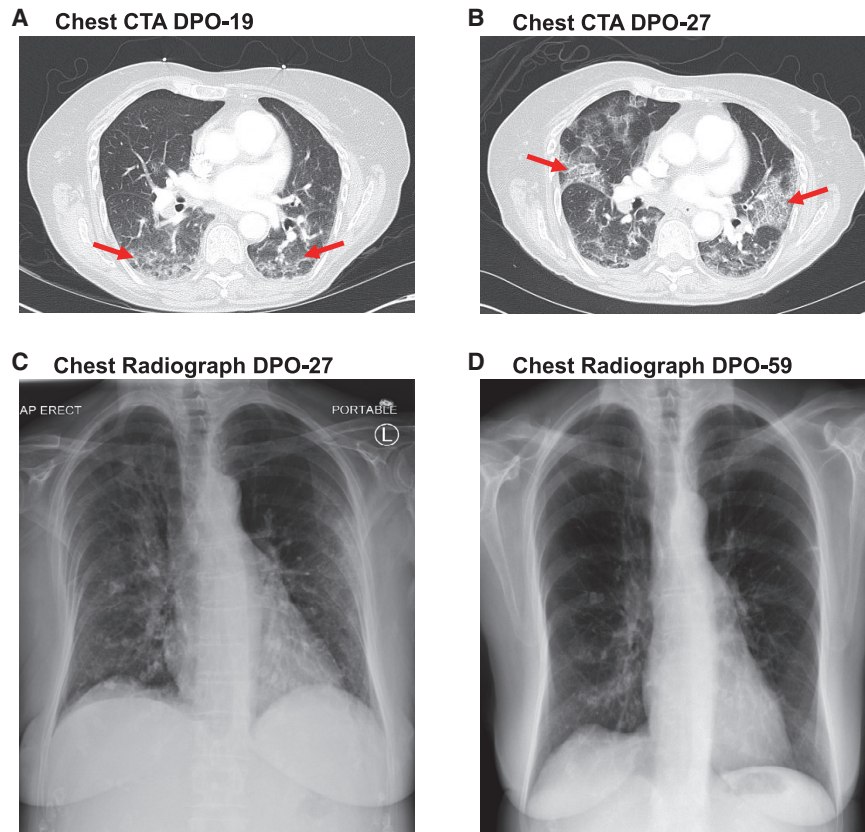


Figure 2. Radiographic analysis of lung abnormalities

(A and B) Computed tomography angiography (CTA) of the chest on the day of initial admission at DPO 19 (A) and subsequent readmission at DPO 27 (B), demonstrating the evolution of diffuse patchy ground glass and interstitial opacities (red arrows in A) consistent with COVID-19 infection to moderately extensive bilateral patchy interstitial lung infiltrates (red arrows in B).

(C and D) An anterior-posterior chest radiograph at DPO 27 (C) demonstrates bilateral patchy interstitial lung infiltrates, which are resolved on a posterior-anterior image at DPO 59 (D). Dense calcified granulomas are old.

received 218 mL (3.6 mL/kg) on DPO 33. She rapidly defervesced over the next 48 h, became SARS-CoV-2 virus negative on DPO 36, was discharged at DPO 37, recovered her weight, and her hepatic function and anemia resolved by DPO 119 (Figures 1A–1D). Repeat chest radiography showed resolution of her pneumonia at DPO 59 (Figure 2D).

Transfer of high-titer neutralizing antibodies has curative potential

Plasma samples from the CLL patient, convalescing relatives 1 and 2, a third unexposed relative (relative 3), and the remnant CP from relative 2 were tested for SARS-CoV-2 anti-S-protein IgG binding Abs by ELISA. High-titer Abs were present in plasma from relatives 1 and 2 as well as in the remnant CP from relative 2 but were absent in relative 3 (Table 1). As expected, anti-S-protein Abs were not initially present in the immunodeficient patient but became detectable 1 day after CP transfusion.

The same plasma samples were then tested for SARS-CoV-2 NABs using an HIV-1-based pseudovirus system.¹⁶ An additional assay for Ab-mediated inhibition of the SARS-CoV-2 RBD/ACE2 interaction generated highly concordant data (Figure S2). Consistent with the ELISA findings, high-titer NABs and ACE2/RBD inhibitory Abs were present in the plasma from relatives 1 and 2 and the remnant CP unit, but not in the pretreatment plasma from the CLL patient (Table 1; Figure S3). However, NABs were clearly detectable on four

consecutive days after CP transfusion with titers consistent with an ~1:10 dilution. Analysis of the CP for receptor binding domain (RBD) reactivity revealed primarily IgG and IgM isotype responses, with IgG1 and IgG3 dominant among the IgG subclasses (Figure S4). The CP contained ~112 µg/mL of RBD-specific IgG1, corresponding to ~24 mg in the transfused unit. Thus, the transfer of a CP unit with a NAb ID₅₀ titer of 5,700 from a convalescent donor to an immunodeficient recipient resulted in the loss of detectable virus in nasal swabs, a dramatic clinical improvement, discharge from the hospital within 4 days, and resolution of an advanced pneumonia (Figures 1 and 2).

Most CP units do not reach pre-transfusion neutralizing antibody levels of hospitalized recipients

To assess how this case compared to other CP transfusions, we measured NAb titers in 38 remnant CP units (RCPUs) from the American Red Cross and other regional blood services that were transfused at UAB under the FDA IND indication for COVID-19 patients (Figure 3).⁵ All CP donors were SARS-CoV-2 PCR or Ab positive and donated plasma at least 14 days after symptom resolution.¹⁷ Only 37% of the RCPUs had NAb titers >250, and only 29% inhibited RBD/ACE2 binding. NABs were undetectable in four RCPUs (ID₅₀ <20). Based on the FDA criterion for ID₅₀ titers >250,¹⁸ a high proportion of these plasmas were inadequate for transfusion. We also analyzed a different set of 26 CP units from LifeSouth Community Blood Centers (LSCPs) that were pre-screened with a SARS-CoV-2 spike immunoassay (Ortho-VITROS). Those CPs were generally of higher titer (median NAb ID₅₀ 456), with 47% exceeding the >250 FDA cutoff and 58% inhibiting ACE2/RBD binding. However, only 8 of the 26 LSCP units had ID₅₀ values >1,000 and none exceeded the 5,700 titer of the CP plasma given to the CLL patient.

To examine how CP transfusion affected plasma NAb activity, we analyzed 17 CP recipients (CPR) for whom pre- and/or post-transfusion blood samples were available. These patients were

Table 1. Anti-S-protein and neutralizing antibodies in plasma from the index case and her relatives

Plasma sample	Collection date (DPO) ^a	SARS-CoV-2 S-Protein IgG ^b		Neutralization (ID ₅₀) ^c	ACE2/RBD binding (1:25) ^d
		EC ₅₀	Endpoint		
Relatives					
Relative 1 (infected daughter)	52	44,770	762,070	6,710	7%
Relative 2 (infected son-in-law/donor)	44	28,350	459,970	13,190	11%
Relative 3 (infection-naive daughter)	–	<100	<100	<20	109%
Remnant convalescent plasma (CP)	38	24,360	266,470	5,720	16%
Index case recipient					
Before CP transfusion (day 0)	33	<100	<100	<20	106%
Day 1 after transfusion	34	1,340	11,680	570	83%
Day 2 after transfusion	35	1,150	12,230	500	89%
Day 3 after transfusion	36	670	12,870	370	98%
Day 4 after transfusion	37	820	12,880	360	102%

^aDPO, days post-onset of symptoms.

^bSARS-CoV-2 IgG S-protein ELISA EC₅₀ and endpoint titers are rounded to the nearest 10, and values of <100 are considered negative.

^cNeutralization ID₅₀ titers are rounded to the nearest 10, and values <20 are considered negative.

^dA reduction in the binding of the angiotensin converting enzyme 2 (ACE2) to the receptor binding domain (RBD) to <90% of control indicates inhibition and values are rounded to the nearest whole number.

hospitalized, mostly in the intensive care unit (Table S1). At baseline, 53% had ID₅₀ values >250, with 7 exceeding titers of 3,000. Overall, the mean ID₅₀ for this cohort before transfusion was 10.2-fold higher than for the RCPD products ($p < 0.001$), 3-fold higher than the LSCP units ($p = 0.003$), and 5.2-fold higher than all units combined ($p < 0.001$) (Figure 3A). Similar results were obtained analyzing ACE2/RBD inhibition (Figure 3B). For 16 CPRs we could analyze, CP transfusion had no significant impact on the pre-existing NAb titers or ACE2/RBD inhibition ($p = 0.50$ and $p = 0.25$, respectively) (Figures 3C and 3D). In contrast, CP transfusion of our CLL patient resulted in an obvious rise in NAb titers (Figures 3A–3D, green samples) to levels that are protective in animal studies.^{19–22}

DISCUSSION

Here, we report the effects of CP immunotherapy in an immunodeficient COVID-19 patient unable to mount a humoral response, who suffered a prolonged deteriorating illness with severe pneumonia and a high risk of death.²³ A single CP transfusion (NAb ID₅₀ 5,700) led to viral clearance, her discharge from the hospital within 4 days, and ultimate resolution of her lung-related pathology. Such a prompt and profound improvement provides compelling evidence for a causative benefit of the transferred NABs. Of note, we saw no indication of an adverse interaction between infused Abs and circulating virus that has been proposed to drive Ab-dependent enhancement and lung pathology.²⁴

Our results have important implications for how CP therapy is being used now and how it may be improved. The low NAB titers in most CP donors raise concerns. The initial FDA guidelines for use of CP as an IND in May 2020 recommended a NAb titers of >160.⁵ According to this criterion, 53% of CPs transfused at UAB exceeded this cutoff. However, the use of CPs with low NAB titers lack demonstrable efficacy.²⁵ Accordingly, the revised

FDA guidance following EUA approval in August 2020 recommended the use of CP with titers >250,¹⁸ indicating that only 36.8% units met this criterion. Although the majority of LSCP samples (85%) had titers >160, only 47% had activity >250. Convalescing individuals with truly high-titer NABs are rare,²⁶ which underscores the need for a concerted effort to identify them but also poses the question of whether there are ample numbers of suitable CP donors.

Our results are consistent with data from other testing centers domestically and abroad. A recent analysis of 753 plasma donors from three different processing centers in the US²⁷ found half maximal neutralization titers (NT₅₀) of >1:160 in 76.4%, >1:320 in 61.6%, and >1:640 in 44.9% of CP units. In contrast, an analysis of CP units in the United Kingdom found NAb titers of >250 in only ~26% of plasma samples ($n = 436$).²⁸ Thus, while more than half of the units collected in the US study had titers >250, it is not yet clear how uniform the distribution of NAB-enriched CP is around the country and, most importantly, what NAb titer threshold provides sufficient efficacy.¹⁰

Our findings confirm the wide disparity in neutralizing activity found for donor plasma in other studies,²⁵ including international randomized controlled clinical trials that failed to find efficacy for CP immunotherapy.^{11,12,29} Thus, beyond reliably identifying suitable high-titer plasma donors, clinical trials that investigate correlates of immune protection will be critical for defining titers more likely to achieve clinical efficacy. In this context, CP studies in non-human primates may also be informative.¹⁹ The evolving FDA guidelines and implementation of improved screening procedures that more accurately define neutralizing activity should improve the CP unit supply quality. However, since NAB levels gradually decline over time,³⁰ retesting will be needed for repeat donations.

The strongest plasma NAB titers are found in the sickest patients, and they increase over time during the first

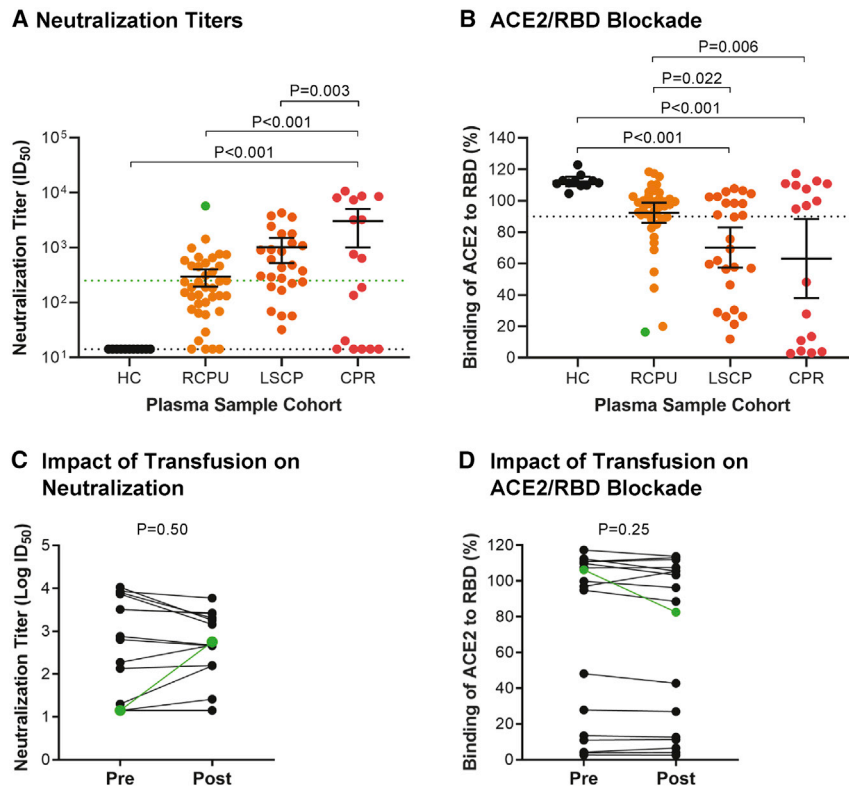


Figure 3. Disparate neutralizing activity of convalescent plasma units and recipients

(A and B) Reciprocal half-maximal pseudovirus NAb titers (A) or ACE2/RBD inhibition at a 1:25 dilution (B) are shown for sera from healthy controls (HC) (n = 11), remnant CP units (RCP) (n = 38), banked LifeSouth CP units (LSCP) (n = 26), and CP recipients (CPR) (n = 17). Bars indicate the mean with 95% confidence intervals (ID₅₀, plasma dilution at which luminescence output was reduced to 50%); dotted black lines indicate assay sensitivity cutoffs, specifically an ID₅₀ value of <20 in the neutralization assay (A) or 90% ACE2 binding in the RBD-inhibition assay (B). The green line in (A) indicates the FDA recommended NAb titer of 250. The p values were calculated by ANOVA with multiple comparisons.

(C and D) A pairwise comparison of log transformed pseudovirus ID₅₀ titers (C) and ACE2/RBD binding (1:25 dilution) titers (D) is shown for 16 CP recipients from whom pre- and post-transfusion plasma samples were available. p values were calculated with a paired Student's t test.

The samples labeled green (A–D) represent the CP unit and CPR samples from the immunodeficient index case patient; they were excluded from the statistical analysis.

~20–30 days after developing symptoms.³¹ Thus, the timing of CP transfusions is another critical consideration given that this treatment is likely to be most effective if given before endogenous NAb development. Indeed, other recent studies have shown that CP therapy may only be beneficial when it is used very early after hospitalization and is enriched with high-titer IgG.^{9–11} Ideally, CP use should consider the NAb titers in both donors and recipients, taking into account the substantial dilution factors involved. The failure to consider these issues may account for why early small-scale CP trials have generated non-definitive outcomes^{11,12,29} and why the recombinant NAb bamlanivimab lacked efficacy in hospitalized COVID-19 patients but may show promise by lowering viral loads in outpatients.³²

While the clinical benefits of CP transfusion may extend beyond NAb, our case demonstrates that CPs with high-titer NAb may be particularly useful to immunocompromised patients. Vaccine efficacy is lower among the immunosuppressed, including those on therapies for transplant rejection, autoimmunity, or cancer.³³ Inadequate humoral responses are a common problem in patients with lymphoproliferative disorders, who develop hypogammaglobulinemia secondary to immune dysregulation or B cell-targeted therapies. An estimated 25%–40% of these patients receive IVIg.³⁴ Thus, passive immunotherapy, including cocktails of monoclonal NAb,^{24,35,36} may be especially important in these populations if they acquire SARS-CoV-2 infection.

In summary, our case report demonstrates that transfusing a high NAb titer CP into a B cell-deficient patient rapidly resolved

her severe COVID-19 illness. CP is a readily available therapeutic option that can potentially provide an immediate benefit. However, the generally low NAb titers in most donors, as well as high-titer baseline NAb in many recipients, highlight the importance of first testing the CPs, and also the recipients. Doing so should optimize the clinical benefit and reduce the effort spent when CP therapy is not appropriate.

Limitations of study

One of the limitations of this report is the sample size of a single index patient. An analysis of neutralizing activity in a larger series of immunodeficient recipients transfused with CP units harboring well-defined NAb titers would be helpful for validating these findings. However, while NAb may serve as a useful correlate of immune protection, the NAb titer threshold required to achieve clinical efficacy still remains unknown. Although the index case was unable to mount a humoral immune response, we did not examine whether the patient developed SARS-CoV-2-specific cell-mediated immunity and whether this contributed to her clinical improvement. Another limitation is that qPCR Ct values of the index case were not available, thus precluding quantitative analyses of SARS-CoV-2 viral loads prior to and after the CP infusion. Finally, we were unable to examine the clinical outcomes of CP recipients who received units with low NAb titers. Thus, it remains unclear whether CP transfusions have beneficial effects in addition to providing Abs capable of neutralizing SARS-CoV-2. These data will ultimately be required to determine the full clinical benefits of CP immunotherapy for COVID-19.

STAR★METHODS

Detailed methods are provided in the online version of this paper and include the following:

- **KEY RESOURCES TABLE**
- **RESOURCE AVAILABILITY**
 - Lead contact
 - Materials availability
 - Data and code availability
- **EXPERIMENTAL MODEL AND SUBJECT DETAILS**
 - Human samples
 - Cell lines
- **METHOD DETAILS**
 - SARS-CoV-2 S-protein ELISA
 - SARS-CoV-2 RBD ELISA
 - SARS-CoV-2 Pseudovirus Neutralization Assay
 - ACE2/RBD Binding Inhibition Assay
- **QUANTIFICATION AND STATISTICAL ANALYSIS**

SUPPLEMENTAL INFORMATION

Supplemental Information can be found online at <https://doi.org/10.1016/j.xcrm.2020.100164>.

ACKNOWLEDGMENTS

We thank the donors and patients who contributed samples to the study as well as Charles Henry, Lorinda Cruz, Christina Morelock, the staff at Sacred Heart Hospital Emerald Coast, and the staff of the UAB blood bank. We also thank Philip Brouwer, Rogier Sanders, Albert Cupo, Wilhem Leconet, and Victor Cruz-Portillo for producing S-proteins. We appreciate Ravi Bhatia, Robert Welner, and Mark Dransfield for helpful discussions. These studies were funded in part by the UAB School of Medicine Dean's office COVID-19 research initiative, the UAB Cancer Immunobiology Program, and NIH/NIAID UM1AI069452, R01AI110553, R01AI036082, and R01AI150590.

AUTHOR CONTRIBUTIONS

Conceptualization, S.L.H., B.H.H., and R.S.D.; Methodology, K.H., T.J.K., T.H., P.D.B., J.P.M., and R.S.D.; Validation, K.H., R.M.R., W.L., and D.T.R.; Formal Analysis, K.H., R.M.R., D.T.R., and R.S.D.; Investigation, K.H., R.M.R., R.L., W.L., R.S., E.M.T., and Y.H.; Resources, L.P., A.N.K., S.S., M.B.M., J.L.L., C.M.L., T.P.M., T.J.K., T.H., P.D.B., J.P.M., P.A.G., S.L.H., and R.S.D.; Writing – Original Draft, R.S.D.; Writing – Review & Editing, M.B.M., J.P.M., P.A.G., S.L.H., B.H.H., and R.S.D.; Supervision, M.B.M., P.A.G., S.L.H., B.H.H., and R.S.D.; Funding Acquisition, J.P.M., P.A.G., S.L.H., B.H.H., and R.S.D.

DECLARATION OF INTERESTS

R.S.D. and K.H. have submitted an intellectual property disclosure related to the ACE2/RBD assay.

Received: August 28, 2020

Revised: October 31, 2020

Accepted: December 1, 2020

Published: December 5, 2020

REFERENCES

1. Casadevall, A., and Pirofski, L.A. (2020). The convalescent sera option for containing COVID-19. *J. Clin. Invest.* *130*, 1545–1548.
2. Casadevall, A., and Scharff, M.D. (1995). Return to the past: the case for antibody-based therapies in infectious diseases. *Clin. Infect. Dis.* *21*, 150–161.
3. Cheng, Y., Wong, R., Soo, Y.O., Wong, W.S., Lee, C.K., Ng, M.H., Chan, P., Wong, K.C., Leung, C.B., and Cheng, G. (2005). Use of convalescent plasma therapy in SARS patients in Hong Kong. *Eur. J. Clin. Microbiol. Infect. Dis.* *24*, 44–46.
4. Arabi, Y.M., Hajeer, A.H., Luke, T., Raviprakash, K., Balkhy, H., Johani, S., Al-Dawood, A., Al-Qahtani, S., Al-Omari, A., Al-Hameed, F., et al. (2016). Feasibility of Using Convalescent Plasma Immunotherapy for MERS-CoV Infection, Saudi Arabia. *Emerg. Infect. Dis.* *22*, 1554–1561.
5. FDA (2020). Coronavirus (COVID-19) update: FDA coordinates national effort to develop blood-related therapies for COVID-19. <https://www.fda.gov/news-events/press-announcements/coronavirus-covid-19-update-fda-coordinates-national-effort-develop-blood-related-therapies-covid-19>.
6. Joyner, M.J., Bruno, K.A., Klassen, S.A., Kunze, K.L., Johnson, P.W., Lesser, E.R., Wiggins, C.C., Senefeld, J.W., Klompas, A.M., Hodge, D.O., et al. (2020). Safety Update: COVID-19 Convalescent Plasma in 20,000 Hospitalized Patients. *Mayo Clin. Proc.* *95*, 1888–1897.
7. Salazar, E., Perez, K.K., Ashraf, M., Chen, J., Castillo, B., Christensen, P.A., Eubank, T., Bernard, D.W., Eagar, T.N., Long, S.W., et al. (2020). Treatment of Coronavirus Disease 2019 (COVID-19) Patients with Convalescent Plasma. *Am. J. Pathol.* *190*, 1680–1690.
8. FDA (2020). Emergency use authorization (EUA) of COVID-19 convalescent plasma for treatment of COVID-19 in hospitalized patients. <https://www.fda.gov/media/141477/download>.
9. Salazar, E., Christensen, P.A., Graviss, E.A., Nguyen, D.T., Castillo, B., Chen, J., Lopez, B.V., Eagar, T.N., Yi, X., Zhao, P., et al. (2020). Treatment of Coronavirus Disease 2019 Patients with Convalescent Plasma Reveals a Signal of Significantly Decreased Mortality. *Am. J. Pathol.* *190*, 2290–2303.
10. Joyner, M.J., Senefeld, J.W., Klassen, S.A., Mills, J.R., Johnson, P.W., Theel, E.S., Wiggins, C.C., Bruno, K.A., Klompas, A.M., Lesser, E.R., et al. (2020). Effect of Convalescent Plasma on Mortality among Hospitalized Patients with COVID-19: Initial Three-Month Experience. *medRxiv*. <https://doi.org/10.1101/2020.08.12.20169359>.
11. Gharbharan, A., Jordans, C.C.E., GeurtsvanKessel, C., den Hollander, J.G., Karim, F., Mollema, F.P.N., Stalenhoef, J.E., Dofferhoff, A., Ludwig, I., Koster, A., et al. (2020). Convalescent Plasma for COVID-19. A randomized clinical trial. *medRxiv*. <https://doi.org/10.1101/2020.07.01.20139857>.
12. Agarwal, A., Mukherjee, A., Kumar, G., Chatterjee, P., Bhatnagar, T., and Malhotra, P.; PLACID Trial Collaborators (2020). Convalescent plasma in the management of moderate covid-19 in adults in India: open label phase II multicentre randomised controlled trial (PLACID Trial). *BMJ* *371*, m3939.
13. Pau, A.K., Aberg, J., Baker, J., Belperio, P.S., Coopersmith, C., Crew, P., Glidden, D.V., Grund, B., Gulick, R.M., Harrison, C., et al. (2020). Convalescent Plasma for the Treatment of COVID-19: Perspectives of the National Institutes of Health COVID-19 Treatment Guidelines Panel. *Ann. Intern. Med.* Published online September 25, 2020. <https://doi.org/10.7326/M20-6448>.
14. Walls, A.C., Park, Y.J., Tortorici, M.A., Wall, A., McGuire, A.T., and Veesler, D. (2020). Structure, Function, and Antigenicity of the SARS-CoV-2 Spike Glycoprotein. *Cell* *181*, 281–292.
15. Hoffmann, M., Kleine-Weber, H., Schroeder, S., Krüger, N., Herrler, T., Erichsen, S., Schiergens, T.S., Herrler, G., Wu, N.H., Nitsche, A., et al. (2020). SARS-CoV-2 Cell Entry Depends on ACE2 and TMPRSS2 and Is Blocked by a Clinically Proven Protease Inhibitor. *Cell* *181*, 271–280.
16. Schmidt, F., Weisblum, Y., Muecksch, F., Hoffmann, H.H., Michailidis, E., Lorenzi, J.C.C., Mendoza, P., Rutkowska, M., Bednarski, E., Gaebler, C., et al. (2020). Measuring SARS-CoV-2 neutralizing antibody activity using pseudotyped and chimeric viruses. *J. Exp. Med.* *217*, e20201181. <https://doi.org/10.1084/jem.20201181>.

17. FDA (2020). Investigational COVID-19 Convalescent Plasma: Guidance for Industry. <https://www.fda.gov/media/136798/download>.
18. FDA (2020). Decisional Memo. <https://www.fda.gov/media/141480/download>.
19. Cross, R.W., Prasad, A.N., Borisevich, V., Woolsey, C., Agans, K.N., Deer, D.J., Dobias, N.S., Geisbert, J.B., Fenton, K.A., and Geisbert, T.W. (2020). Use of convalescent serum reduces severity of COVID-19 in nonhuman primates. *bioRxiv*. <https://doi.org/10.1101/2020.10.14.340091>.
20. Sun, J., Zhuang, Z., Zheng, J., Li, K., Wong, R.L., Liu, D., Huang, J., He, J., Zhu, A., Zhao, J., et al. (2020). Generation of a Broadly Useful Model for COVID-19 Pathogenesis, Vaccination, and Treatment. *Cell* **182**, 734–743.
21. Rogers, T.F., Zhao, F., Huang, D., Beutler, N., Burns, A., He, W.T., Limbo, O., Smith, C., Song, G., Woehl, J., et al. (2020). Isolation of potent SARS-CoV-2 neutralizing antibodies and protection from disease in a small animal model. *Science* **369**, 956–963.
22. Zheng, J., Wong, L.R., Li, K., Verma, A.K., Ortiz, M., Wohlford-Lenane, C., Leiding, M.R., Knudson, C.M., Meyerholz, D.K., McCray, P.B., Jr., and Perlman, S. (2020). COVID-19 treatments and pathogenesis including anosmia in K18-hACE2 mice. *Nature*, Published online November 8, 2020. <https://doi.org/10.1038/s41586-020-2943-z>.
23. Mato, A.R., Roeker, L.E., Lamanna, N., Allan, J.N., Leslie, L., Pagel, J.M., Patel, K., Osterborg, A., Wojenski, D., Kamdar, M., et al. (2020). Outcomes of COVID-19 in patients with CLL: a multicenter international experience. *Blood* **136**, 1134–1143.
24. Klasse, P.J., and Moore, J.P. (2020). Antibodies to SARS-CoV-2 and their potential for therapeutic passive immunization. *eLife* **9**, e57877.
25. Bradfute, S.B., Hurwitz, I., Yingling, A.V., Ye, C., Cheng, Q., Noonan, T.P., Raval, J.S., Sosa, N.R., Mertz, G.J., Perkins, D.J., and Harkins, M.S. (2020). Severe Acute Respiratory Syndrome Coronavirus 2 Neutralizing Antibody Titers in Convalescent Plasma and Recipients in New Mexico: An Open Treatment Study in Patients With Coronavirus Disease 2019. *J. Infect. Dis.* **222**, 1620–1628.
26. Robbiani, D.F., Gaebler, C., Muecksch, F., Lorenzi, J.C.C., Wang, Z., Cho, A., Agudelo, M., Barnes, C.O., Gazumyan, A., Finkin, S., et al. (2020). Convergent antibody responses to SARS-CoV-2 in convalescent individuals. *Nature* **584**, 437–442.
27. Goodhue Meyer, E., Simmons, G., Grebe, E., Gannett, M., Franz, S., Darst, O., Di Germanio, C., Stone, M., Contestable, P., Prichard, A., et al. (2020). Selecting COVID-19 Convalescent Plasma for Neutralizing Antibody Potency Using a High-capacity SARS-CoV-2 Antibody Assay. *medRxiv*. <https://doi.org/10.1101/2020.08.31.20184895>.
28. Harvala, H., Mehew, J., Robb, M.L., Ijaz, S., Dicks, S., Patel, M., Watkins, N., Simmonds, P., Brooks, T., Johnson, R., et al. (2020). Convalescent plasma treatment for SARS-CoV-2 infection: analysis of the first 436 donors in England, 22 April to 12 May 2020. *Euro Surveill.* **25**, 2001260.
29. Li, L., Zhang, W., Hu, Y., Tong, X., Zheng, S., Yang, J., Kong, Y., Ren, L., Wei, Q., Mei, H., et al. (2020). Effect of Convalescent Plasma Therapy on Time to Clinical Improvement in Patients With Severe and Life-threatening COVID-19: A Randomized Clinical Trial. *JAMA* **324**, 460–470.
30. Wang, K., Long, Q.X., Deng, H.J., Hu, J., Gao, Q.Z., Zhang, G.J., He, C.L., Huang, L.Y., Hu, J.L., Chen, J., et al. (2020). Longitudinal dynamics of the neutralizing antibody response to SARS-CoV-2 infection. *Clin. Infect. Dis.*, [ciaa1143](https://doi.org/10.1093/cid/ciaa1143).
31. Wang, X., Guo, X., Xin, Q., Pan, Y., Hu, Y., Li, J., Chu, Y., Feng, Y., and Wang, Q. (2020). Neutralizing Antibodies Responses to SARS-CoV-2 in COVID-19 Inpatients and Convalescent Patients. *Clin. Infect. Dis.*, [ciaa721](https://doi.org/10.1093/cid/ciaa721).
32. Chen, P., Nirula, A., Heller, B., Gottlieb, R.L., Boscia, J., Morris, J., Huhn, G., Cardona, J., Mocherla, B., Stosor, V., et al.; BLAZE-1 Investigators (2020). SARS-CoV-2 Neutralizing Antibody LY-CoV555 in Outpatients with Covid-19. *N. Engl. J. Med.* Published online October 28, 2020. <https://doi.org/10.1056/NEJMoa2029849>.
33. Kunisaki, K.M., and Janoff, E.N. (2009). Influenza in immunosuppressed populations: a review of infection frequency, morbidity, mortality, and vaccine responses. *Lancet Infect. Dis.* **9**, 493–504.
34. Na, I.K., Buckland, M., Agostini, C., Edgar, J.D.M., Friman, V., Michallet, M., Sánchez-Ramón, S., Scheibenbogen, C., and Quinti, I. (2019). Current clinical practice and challenges in the management of secondary immunodeficiency in hematological malignancies. *Eur. J. Haematol.* **102**, 447–456.
35. Pinto, D., Park, Y.J., Beltramello, M., Walls, A.C., Tortorici, M.A., Bianchi, S., Jaconi, S., Culap, K., Zatta, F., De Marco, A., et al. (2020). Cross-neutralization of SARS-CoV-2 by a human monoclonal SARS-CoV antibody. *Nature* **583**, 290–295.
36. Baum, A., Ajithdoss, D., Copin, R., Zhou, A., Lanza, K., Negron, N., Ni, M., Wei, Y., Mohammadi, K., Musser, B., et al. (2020). REGN-COV2 antibodies prevent and treat SARS-CoV-2 infection in rhesus macaques and hamsters. *Science* **370**, 1110–1115.
37. Accelerated emergency use authorization (EUA) summary FRL SARS-CoV-2 Test (UAB Fungal Reference Lab). <https://www.fda.gov/media/139437/download>.
38. Bryan, A., Pepper, G., Wener, M.H., Fink, S.L., Morishima, C., Chaudhary, A., Jerome, K.R., Mathias, P.C., and Greninger, A.L. (2020). Performance Characteristics of the Abbott Architect SARS-CoV-2 IgG Assay and Sero-prevalence in Boise, Idaho. *J. Clin. Microbiol.* **58**, e00941-20.
39. Brouwer, P.J.M., Caniels, T.G., van der Straten, K., Snitselaar, J.L., Aldon, Y., Bangaru, S., Torres, J.L., Okba, N.M.A., Claireaux, M., Kerster, G., et al. (2020). Potent neutralizing antibodies from COVID-19 patients define multiple targets of vulnerability. *Science* **369**, 643–650.

STAR★METHODS

KEY RESOURCES TABLE

REAGENT or RESOURCE	SOURCE	IDENTIFIER
Antibodies		
Goat anti-human IgG Fc-HRP	SouthernBiotech	Cat# 2048-05; RRID: AB_2795688
Goat anti-human IgG-HRP	SouthernBiotech	Cat# 2045-05; RRID:AB_2795676
Goat anti-human IgM-HRP	SouthernBiotech	Cat# 2023-05; RRID:AB_2795622
Goat anti-human IgA-HRP	SouthernBiotech	Cat# 2053-05; RRID:AB_2795715
Mouse anti-human IgG1-HRP (clone HP6069)	Invitrogen	Cat# A-10648; RRID:AB_2534051
Mouse anti-human IgG1- HRP (clone 4E3)	SouthernBiotech	Cat# 9052-05; RRID:AB_2796619
Mouse anti-human IgG2-HRP (clone 31-7-4)	SouthernBiotech	Cat# 9060-05; RRID:AB_2796633
Mouse anti-human IgG3-HRP (clone HP6050)	SouthernBiotech	Cat# 9210-05; RRID:AB_2796699
Mouse anti-human IgG4-HRP (clone HP6025)	SouthernBiotech	Cat# 9200-05; RRID:AB_2796691
Mouse anti-human IgA1- HRP (clone B3506B4)	Southern Biotech	Cat# 9130-05; RRID:AB_2796654
Goat anti-human ACE2-biotin	R&D systems	Cat# BAF933; RRID:AB_2305177
Human IgG1 anti-Spike-RBD (clone CR3022)	Obtained from the lab of Dr. James Kobie	
Human IgM anti-Spike-RBD-hIgM (clone CR3022)	Invivogen	Cat# srbd-mab5
Human IgA1 anti-Spike-RBD-hIgA1 (clone CR3022)	Invivogen	Cat# srbd-mab6
Bacterial and virus strains		
MAX Efficiency Stbl2 Competent Cells	ThermoFisher	Cat# 10268019
Biological samples		
Human serum	Millipore Sigma	Cat# H5667
Chemicals, peptides, and recombinant proteins		
3,3',5,5'-Tetramethylbenzidine (TMB) Liquid Substrate	Sigma-Aldrich	Cat# T0440-1L
3,3',5,5'-Tetramethylbenzidine (TMB)	BioLegend	Cat# 421501
Sulfuric Acid (1N)	ICCA	Cat# 8300-32
SARS CoV2 His-tag	Brouwer et al., Produced In House	PMID: 32540902
SARS Cov2 Strep-tag	Brouwer et al., Produced In House	PMID: 32540902
SARS CoV2 Avi-tag	Brouwer et al., Produced In House	PMID: 32540902
Recombinant human ACE2	Raybiotech	Cat# 230-30165
Recombinant SARS-CoV-2 S1 subunit (RBD)	Raybiotech	Cat# 230-30162
DMEM	ThermoFisher	Cat# 10566024
Characterized Fetal Bovine Serum, US Origin	HyClone	Cat# SH30071.02
Penicillin-Streptomycin-Glutamine (100X)	ThermoFisher	Cat# 10378016
FuGENE 6 Transfection Reagent	Promega	Cat# E2692

(Continued on next page)

Continued		
REAGENT or RESOURCE	SOURCE	IDENTIFIER
Critical commercial assays		
Nano-Glo Luciferase Assay System	Promega	Cat# N1150
SARS-CoV-2 IgG	Abbott Laboratories	Cat# 6R86
Experimental models: cell lines		
Human embryo kidney (HEK) 293T cells	ATCC	ATCC CRL-3216
293T-ACE2-Clone13	Schmidt et al.	PMID: 32692348
Recombinant DNA		
pHIV-1 _{NL4ΔEnv} -NanoLuc	Schmidt et al.	PMID: 32692348
pSARS-CoV-2-S _{Δ19}	Schmidt et al.	PMID: 32692348
Software and algorithms		
Graphpad Prism version 8	Graphpad	https://www.graphpad.com:443/
Other		
Corning Clear Polystyrene 96-Well Microplates	FisherScientific	Cat# 07-200-642
Corning 96-Well, High Binding, Flat-Bottom, Half-Area Microplate	FisherScientific	Cat# 07-200-37
Streptavidin-HRP	SouthernBiotech	Cat# 7105-05

RESOURCE AVAILABILITY

Lead contact

Further information and requests for resources and reagents should be directed to and will be fulfilled by the Lead Contact, Randall S. Davis (rsdavis@uab.edu).

Materials availability

This study did not generate new unique reagents.

Data and code availability

This study did not generate any unique datasets or code.

EXPERIMENTAL MODEL AND SUBJECT DETAILS

Human samples

Blood samples were collected following institutional review board (IRB) approval by the University of Alabama at Birmingham (IRB #130821005 and 160125005) and written informed consent was obtained from all participants including the index patient (72 year old female) and relatives (Relative 1, 50 year old female; Relative 2, 58 year old male; and Relative 3, 53 year old female) (Table 1). Diagnosis of SARS-CoV-2 infection was determined by real-time polymerase-chain-reaction (PCR) analysis of respiratory swab specimens³⁷ and/or detection of nucleocapsid IgG antibodies in the blood (Abbott)³⁸ performed in a clinical diagnostic laboratory. Seronegative healthy controls (n = 11) were obtained from cryopreserved samples prior to Dec 31, 2020. Sera from CP recipients (n = 16) and units (n = 38) was obtained from remnant blood specimens or discarded plasma bags and tubing. Details of the gender and age for CP recipients is provided in Table S1. Deidentified samples from banked SARS-CoV-2 recovered donor CP units (n = 26) were obtained from LifeSouth Blood Bank (Gainesville, FL).

Cell lines

HEK293T (ATCC) and 293T-ACE2-Clone13 cells were cultured in DMEM supplemented with 10% fetal bovine serum, L-glutamine, and penicillin/streptomycin at 37°C and 5% CO₂.

METHOD DETAILS

SARS-CoV-2 S-protein ELISA

The design of the soluble, His-tagged, stabilized SARS-CoV-2 spike (S)-protein (residues 1-1138 of the Wuhan strain) has been described previously.³⁹ Test wells of Corning Clear Polystyrene 96-Well Microplates (FisherScientific #07-200-642) were coated

with 300 ng of S-protein in PBS (100 μ l) overnight at 4°C. All subsequent incubation steps were carried out at 37°C in volumes of 100 μ l. The plates were blocked with blocking buffer (5% non-fat milk powder in PBS + 0.05% Tween 20) for 1 h incubation. Plasma samples were 5-fold serially diluted in blocking buffer and added to the plates for 1 h incubation. Plates were then washed five times with washing buffer (PBS + 0.1% Tween 20) and incubated for 1 h with a goat anti-human IgG horseradish peroxidase (HRP) conjugated antibody (SouthernBiotech #2048-05) diluted 1:5,000 in blocking buffer. Plates were again washed five times with washing buffer. For color development, the TMB substrate (Sigma-Aldrich #T0440-1L) was added for 10 min before the reaction was stopped with an equal volume of 1N H₂SO₄. Absorbance was read at 450 nm using a Synergy 4 (BioTek) spectrophotometer. For each serum dilution, the average OD₄₅₀ value from three background control wells (no serum) was subtracted from the S-protein coated sample wells. In addition, the average OD₄₅₀ value plus 2 standard deviation derived from 28 pre-pandemic sera from UAB was subtracted for each serum dilution. Midpoint (EC₅₀) values were calculated by a nonlinear-regression fit of a 4-parameter sigmoid function to the corrected OD₄₅₀ values and the logarithmic dilution factors (the lower plateau was set to 0; GraphPad Prism software). The end-point titers were read from the fitted curve at a corrected OD₄₅₀ cut-off of 0.1.

SARS-CoV-2 RBD ELISA

High-binding 96-well plates (Corning #3690) were coated at 4°C overnight with 50 μ l of recombinant RBD (RayBiotech) diluted at 1 μ g/ml in PBS. The following day, plates were washed 3 times with 0.1% Tween 20 in PBS (PBST). A blocking solution of 100 μ l per well of 3% non-fat dry milk in PBST was added and incubated at room temperature for 1 h, before washing plates 3 times with PBST. Plasma samples were inactivated at 56°C for 30 min and initially diluted at 1:25, then serially diluted 4-fold in 1% non-fat dry milk in PBST before adding 50 μ l per well, and incubating at room temperature for 2 h. Plates were then washed 3 times with PBST, and a 50 μ l per well mixture of horseradish peroxidase (HRP) conjugated goat anti-human IgG (1:8000), goat anti-human IgM (1:10000), goat anti-human IgA (1:5000), mouse anti-human IgG1 (clone 4E3, 1:1000), mouse anti-human IgG2 (31-7-4, 1:500), mouse anti-human IgG3 (HP6050, 1:4000), or mouse anti-human IgG4 (HP6025, 1:3000) (all from Southern Biotech) in PBST was added to the wells and incubated at room temperature for 1 h to measure S-RBD Ab responses. For quantitative measurements of RBD-specific antibodies, 50 μ l of serially diluted human IgG1 anti-Spike-RBD (clone CR3022, a gift from Dr. James Kobie), human IgM anti-Spike-RBD (CR3022, Invitrogen), and human IgA1 anti-Spike-RBD (CR3022, Invitrogen) in 1% non-fat dry milk in PBST were used as standards, and plate bound Abs were detected by HRP conjugated goat anti-human IgM (1:20000, Southern Biotech), mouse anti-human IgG1 (HP6069, 1:750, Invitrogen), and mouse anti-human IgA1 (B3506B4, 1:1200, Southern Biotech) in PBST, respectively. Plates were washed 4 times with PBST, developed with 50 μ l per well of HRP substrate 3, 3', 5, 5' tetramethyl benzidine (TMB, Biolegend) at room temperature for 10 min. The reaction was stopped by addition of 50 μ l of 1N H₂SO₄. The optical density (OD) was measured at 450 nm with a SPECTROstar omega (BMG Labtech) microplate reader. EC₅₀ values and endpoints were determined as detailed for the SARS-CoV-2 S-protein ELISA.

SARS-CoV-2 Pseudovirus Neutralization Assay

Plasma samples were tested for SARS-CoV-2 neutralizing antibodies as previously described.¹⁶ Briefly, pseudovirus was generated by co-transfection in HEK293T cells, using an HIV-1 nanoluciferase reporter construct and an expression plasmid for the SARS-CoV-2 Spike (Wuhan 1), containing a 19-amino acid cytoplasmic tail truncation. To test neutralization, 1.5x10⁴ 293T-ACE2 cells (clone 13) were seeded in 96-well plates. The following day, five-fold serial dilutions of plasma were incubated with pseudovirus for one hour at 37°C prior to the addition to target cells. Two days post infection, cells were washed with PBS, lysed, and nanoluciferase activity was determined according to manufacturer's instructions (Nano-Glo Luciferase Assay System). Luciferase activity in wells with virus and no patient plasma were set to 100%, and the dilution of plasma at which luminescence was reduced to 50% (ID₅₀) was calculated.

ACE2/RBD Binding Inhibition Assay

Plasma samples were analyzed with an ACE2/receptor binding domain (RBD) binding inhibition assay. High-binding 96-well plates (Corning #3690) were coated with 50 μ l per well of recombinant RBD (RayBiotech) diluted at 1 μ g/ml in PBS at 4°C overnight. The following day, plates were washed 3 times with PBS + 0.1% Tween 20 (PBST), and wells were blocked with 100 μ l per well of 3% non-fat dry milk in PBST by incubation at room temperature for 1 h. After washing the blocked wells 3 times with PBST, either 50 μ l of serum or plasma samples serially diluted in 1% non-fat dry milk in PBST, or 1% non-fat dry milk in PBST alone as a no inhibition control, was added to wells, and incubated at room temperature for 2 h. Heat-inactivated plasma samples (56°C for 30 min) were initially diluted at 1:25, then serially diluted 2-fold for the assay to 1:400. After incubation, plates were washed 3 times with PBST, then 50 μ l per well of recombinant human ACE2 (RayBiotech) diluted at 0.1 μ g/ml in PBST was added to the wells. Plates were incubated at room temperature for 1 h, washed 4 times with PBST, and 50 μ l per well of biotinylated goat anti-human ACE2 (R&D) diluted at 0.1 μ g/ml in PBST was added to wells. Plates were incubated at room temperature for 1 h, washed 4 times with PBST, and then 50 μ l per well of HRP-conjugated streptavidin (Southern Biotech) (1:2000 in PBST) was added to the wells, and incubated at room temperature for 30 min. Plates were washed 5 times with PBST, developed with 50 μ l per well of 3,3',5,5'-tetramethylbenzidine TMB substrate (Biolegend) at room temperature for 8 min, and the reaction was stopped by addition of 50 μ l of 1N H₂SO₄. The OD was measured at 450 nm with a SPECTROstar omega (BMG Labtech) microplate reader. ACE2 binding was expressed as a percentage of OD values relative to OD value of a no inhibition control. Binding values of < 90% at a 1:25 dilution of plasma were used to calculate inhibitory activity.

QUANTIFICATION AND STATISTICAL ANALYSIS

Statistical analysis was performed and visualized using GraphPad Prism v8 software. Correlations between ACE2/RBD binding (1:25 dilution) and neutralization activity (ID_{50}) were analyzed using the Pearson correlation coefficient. Comparisons among plasma sample cohorts were analyzed by ANOVA with Tukey's multiple comparisons and Brown-Forsythe test correction. Comparisons between CP recipients pre and post transfusion were analyzed with Student's paired t test. Statistical parameters are provided in [Figure S2](#) and [Figure 3](#). P values below 0.05 were considered significant.